



Microwave photoconductance decay measurements of n- and p-type silicon irradiated with neutrons and protons

Hani Baek ^{a,b}, Gihyun Kwon ^b, Jongsuk Nam ^b, Sangeun Kim ^{a,b}, Hyoungtaek Kim ^a, Byung-Gun Park ^a, Jungil Lee ^a, Minyong Kang ^{a,***}, Gwang Min Sun ^{a,**}, Chansun Shin ^{b,*}

^a Korea Atomic Energy Research Institute, Daejeon, 34057, Republic of Korea

^b Department of Materials Science and Engineering, Myongji University, Yongin, 17058, Republic of Korea



ARTICLE INFO

Keywords:
 Recombination lifetime
 Microwave photoconductance decay method
 Neutron irradiation
 Proton irradiation
 Silicon

ABSTRACT

N-type and p-type silicon were irradiated by neutrons and protons from low to high fluence range ($10^8 - 10^{11}$ cm $^{-2}$ for neutrons and $10^{10} - 10^{13}$ cm $^{-2}$ for protons). The carrier recombination lifetime of each irradiated silicon was measured using a microwave photoconductance decay method, and the resistivity of the irradiated silicon was also measured. Both neutron and proton irradiation induced a similar lifetime at the same irradiation fluence. The defect formation rates were determined to vary with irradiation fluence from the inverse lifetime dependence on irradiation fluence. The sheet resistance was increased above a threshold fluence. The result shows that at least three different values of defect formation rate are present in the fluence range of $10^9 - 10^{15}$ cm $^{-2}$, and it may have potential for practical use as low-dose dosimeters.

1. Introduction

The minority carrier lifetime (recombination lifetime) is defined as the average existence time of optically or electrically excited minority carriers before they recombine with majority carriers. The lifetime of a semiconductor wafer is sensitive to impurities and crystal defects in the wafer (Schroder, 1997). Hence, measurements of the lifetime are often used for monitoring semiconductor manufacturing processes. The measurement also plays an important role in the characterization of the wafers used in the preparation of power semiconductors and photovoltaic devices (Eikelboom et al., 1995). A short lifetime is desirable for a power semiconductor device that requires a high switching rate and fast recovery, whereas a long lifetime is advantageous for photovoltaic solar cells to increase the charge collection efficiency.

Irradiation with high-energy particles, such as electrons, protons, and neutrons, generates crystal defects in semiconductor wafers and devices (Huhtinen et al., 2002). Irradiation-induced defects affect not only the recombination lifetime (Brotherton and Bradley, 1982) but also the resistivity of semiconductors (Liao et al., 2003; Abbaci et al., 2006). Thus, fine tuning of irradiation has been considered a possible way to optimize the performance of semiconductor devices. High-voltage and

high-frequency power semiconductor devices, for example, can be produced by fast neutron irradiation and post-irradiation annealing (Bin et al., 1993).

A series of studies have been conducted to investigate the effects of irradiation on the recombination lifetime of Si wafers in the proton fluence range of $10^9 - 4 \times 10^{10}$ cm $^{-2}$ and $5 \times 10^{12} - 10^{15}$ cm $^{-2}$ (Gaubas et al., 2005) and in the neutron fluence range of $10^{12} - 3 \times 10^{16}$ cm $^{-2}$ (Gaubas et al., 2008). The lifetime was found to decrease as irradiation fluence increases, and neutron and proton irradiation have quantitatively similar effects, indicating that similar types of radiation defects are generated. Electron irradiation shows the same decreasing lifetime trend, but the absolute lifetime values were significantly different from neutron and proton irradiation (Višniakov et al., 2008). The deep-level transient spectroscopy (DLTS) was employed to examine deep levels spectra generating lifetime variations with irradiation fluence and particle species (Višniakov et al., 2008; Gaubas et al., 2010).

The recombination lifetime in wafers was measured using microwave photoconductance decay (μ -PCD) in these studies, as well as in many recent studies. The μ -PCD method provides a contactless measurement of the recombination lifetime of free carriers in semiconductors following a pulse of optical excitation (Basore and Hansen,

* Corresponding author.

** Corresponding author.

*** Corresponding author.

E-mail addresses: kangmy@kaeri.re.kr (M. Kang), gmsun@kaeri.re.kr (G.M. Sun), c.shin@mju.ac.kr (C. Shin).

1990) and has been widely used to provide a simple and reliable measurement of the recombination lifetime in wafers (Väinölä et al., 2005; Kumar et al., 2007; Lauer et al., 2008).

In this work, carrier lifetimes as well as resistivity were evaluated for both n- and p-type Si wafers irradiated by neutrons and protons in the fluence range of 10^8 – 10^{11} cm $^{-2}$ and 10^{10} – 10^{13} cm $^{-2}$, respectively. A systematic comparison between n- and p-type silicon has yet been published, especially in these fluence range. A possible practical application of this study is discussed in this study.

2. Material and methods

Commercial n-phosphorous and p-boron-doped Czochralski Si (100) wafers with initial resistivity 1–10 Ω cm and a diameter of 100 mm and thickness of 525 μm were used for neutron irradiation. The oxygen and carbon concentrations were 10–18 ppm and less than 1 ppm, respectively. For proton irradiation, Si wafers were diced into Si samples with dimensions of 10 × 10 mm.

Neutron irradiation was performed at ambient temperature (~25 °C) by using neutrons produced by bombarding a beryllium target with 30 MeV protons accelerated by the MC-50 cyclotron at the Korea Institute of Radiological Medical Sciences (Shin et al., 2015). Neutrons with various energies up to 30 MeV were produced. The energy spectrum of neutrons can be found by Baek et al. (2017). The neutron fluence was in the range of 10^8 – 10^{11} cm $^{-2}$, with a flux of 10 8 cm $^{-2}$ ·s $^{-1}$. Proton irradiation with 10 MeV protons was performed using the MC-50 cyclotron. The proton fluence was in the range of 10^{10} – 10^{13} cm $^{-2}$. The proton flux

was approximately 10 11 cm $^{-2}$ ·s $^{-1}$. Insulated gate bipolar transistor (IGBT) devices packaged in a TO-3 package were placed 20 cm in front of Si wafers during neutron irradiation. The purpose of this experimental setup is to evaluate the effect of neutron interaction with semiconductor devices on the lifetime changes of neutron-irradiated Si wafers, which can be taken advantage of in dosimeters.

Mapping of carrier lifetime was conducted for unirradiated and irradiated silicon by Semilab WT-2000 μ-PCD. The mapping used a laser with a wavelength of 904 nm and a pulse width of 200 ns to generate excess carriers. The power of the laser was remained constant during the measurements. The laser-excited area was approximately 1 mm 2 and probed with microwaves of ~10.3 GHz frequency. The PCD measurement is made in less than 1 s per measurement point of the 1 mm 2 area. The lifetimes from the entire Si wafer could be mapped to approximately 24 min.

The resistivity of the unirradiated and neutron-irradiated Si wafers was measured using eddy current measurements equipped in the WT-200 μ-PCD. For proton-irradiated Si samples, the eddy current measurement was not possible owing to sample size limitation. Hence, the sheet resistance was measured using the four-point probe method. Further, the sheet resistance of neutron-irradiated n-type Si was measured for comparison with proton-irradiated data.

3. Results and discussion

Fig. 1(a) shows the spatial lifetime mapping of n-type and p-type Si wafers measured prior to neutron irradiation. Concentric rings can be

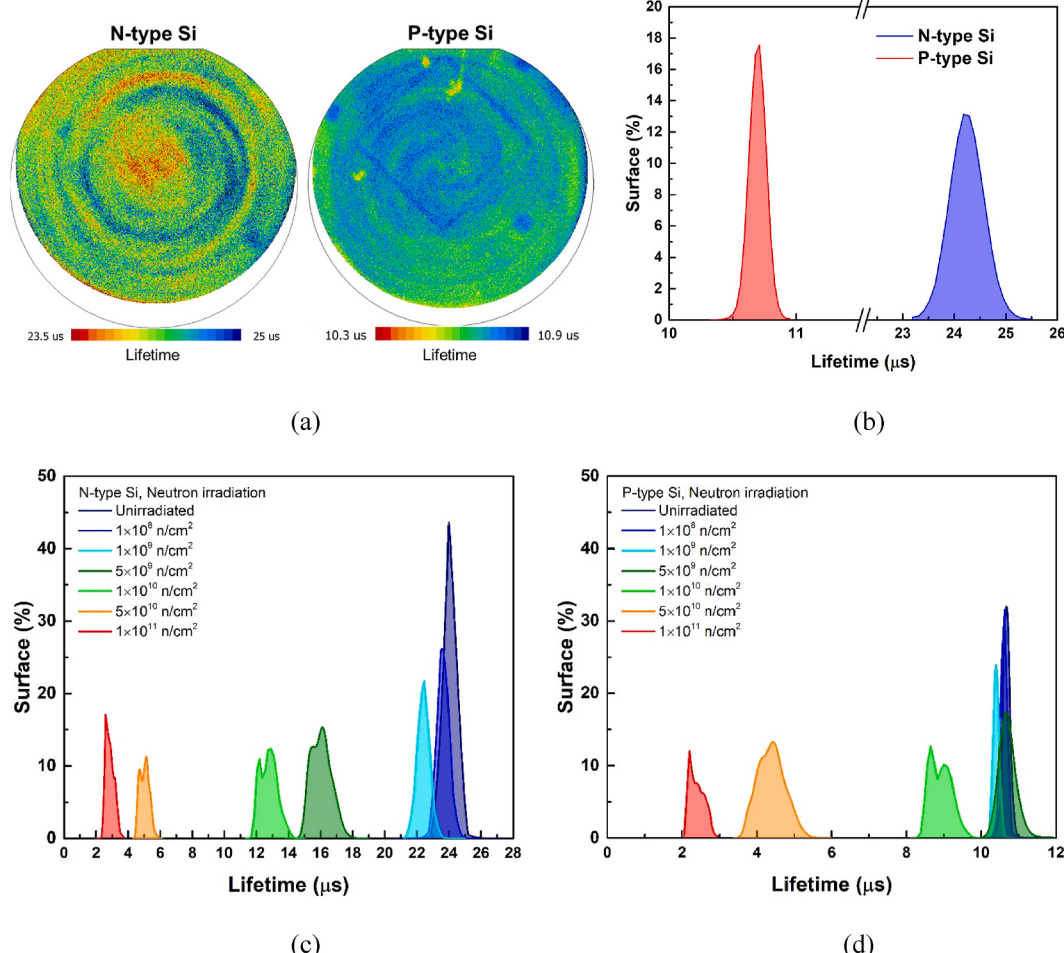
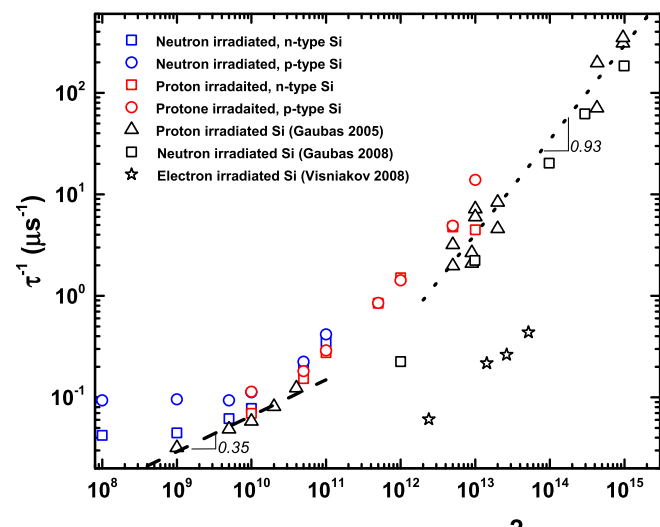


Fig. 1. (a) μ-PCD lifetime mapping. (b) Lifetime histograms measured before neutron irradiation. Lifetime histograms of neutron-irradiated (c) n-type and (d) p-type Si wafers.

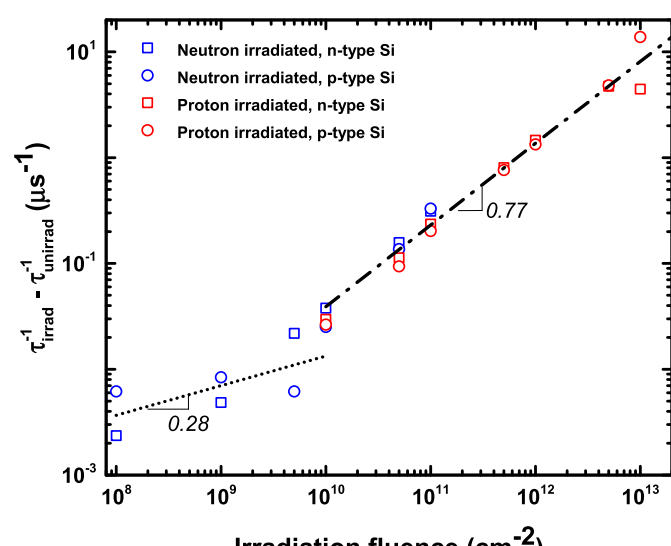
observed on both Si wafers, which are characteristic of Czochralski silicon induced by inhomogeneous distribution of impurities (Rougieux et al., 2019). The histograms shown in Fig. 1(b) indicate quite uniform variations in the lifetime over the entire surface of both n- and p-type Si wafers. The lifetime of the n-type Si wafer ($24.27 \pm 0.34 \mu\text{s}$) is greater than that of the p-type Si wafer ($10.72 \pm 0.68 \mu\text{s}$). Note that Si wafers passivated with thick thermal oxide films showed lifetime values of $\sim 200 \mu\text{s}$ (Gaubas et al., 2005) much higher than those of the as-received (native oxide coated) wafers used in this study.

The histograms of neutron-irradiated Si wafers are shown in Fig. 1(c) and (d) for n- and p-type Si, respectively. The histograms overlap at fluences less than $1 \times 10^9 \text{ cm}^{-2}$ but shift to the left at higher neutron fluences for both types of Si wafers. The measured lifetime using the μ -PCD method is an effective lifetime, which is a combination of lifetimes associated with recombination processes in both the sample surface and the bulk (Cuevas and Macdonald, 2004). As will be shown later in Fig. 3(a), the lifetimes obtained in the irradiated Si wafers in this study nearly coincide with those measured in proton- and neutron-irradiated Si wafers with thick thermal oxide films (Gaubas et al., 2005; 2008; Višniakov et al., 2008). Hence, the measured lifetimes of the irradiated Si wafers seem not to be dominated by surface recombination.

Fig. 2(a) shows the depth profiles of vacancies produced by 10-MeV protons and deposited protons inside Si, which were calculated using the

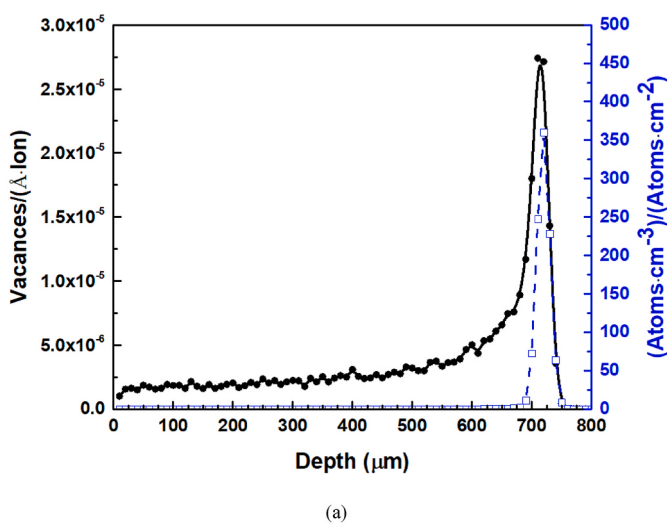


(a)

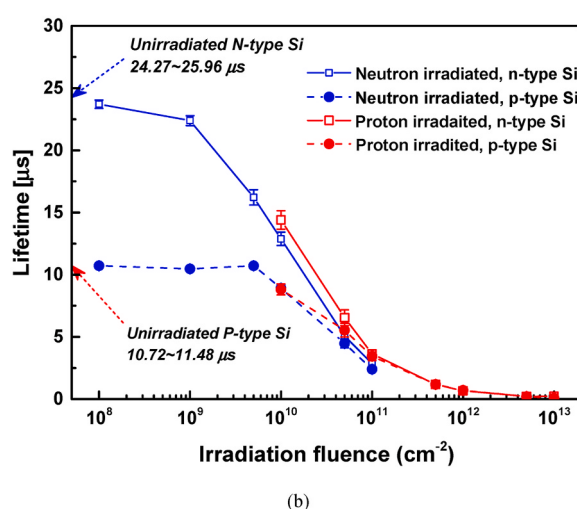


(b)

Fig. 3. (a) Lifetime variations with irradiation fluence and (b) difference in lifetimes of n- and p-type Si as a function of irradiation fluence.



(a)



(b)

Fig. 2. (a) Vacancy and deposited proton profile calculated by SRIM for 10 MeV protons in Si and (b) lifetime mapping of proton-irradiated Si samples with a dimension of $10 \times 10 \text{ mm}$.

SRIM code (Ziegler et al., 1985). As shown in Fig. 2(a), 10-MeV protons stop at a depth of $\sim 750 \mu\text{m}$ and introduce a rather homogeneous distribution of vacancies up to a depth of $\sim 500 \mu\text{m}$. Hence, proton irradiation can be thought to penetrate the entire depth of 525- μm -thick Si wafers and form homogeneously distributed defects within the wafers. During the μ -PCD measurements, the laser produces an initial carrier distribution of $\sim 30\text{-}\mu\text{m}$ deep (Fujihira et al., 1993). The electron-hole pairs injected by a laser will recombine with these homogeneous defects introduced by proton irradiation. Neutrons are also expected to introduce homogeneous distributions of defects within thickness of Si wafers because neutrons have a larger penetration depth in matter than protons due to its electrical neutrality.

Fig. 2(b) shows that the lifetimes of neutron- and proton-irradiated n- and p-type silicon decrease with increasing irradiation fluence. The lifetimes measured in neutron-irradiated Si wafers coincide well with those measured in proton-irradiated Si samples in the fluence range of $10^{10} - 10^{11} \text{ cm}^{-2}$. At a higher fluence range of $10^{11} - 10^{13} \text{ cm}^{-2}$, the

difference between n-type and p-type Si wafers is hardly discernible. The decrease in lifetimes with an irradiation fluence relates to the formation of radiation-induced defects, which act as recombination centers. The coincidence of lifetimes for neutron- and proton-irradiated Si was also observed in other study and indicates that high-energy protons and neutrons induce similar prevailing recombination centers in Si wafers (Gaubas et al., 2008).

In order to better understand defect formation rates in different fluence ranges, the reciprocal lifetimes τ^{-1} as a function of irradiation fluence (Φ) are shown in Fig. 3(a) along with the data of proton-irradiated Si wafers in the fluence range of $10^9 - 4 \times 10^{10} \text{ cm}^{-2}$ and $5 \times 10^{12} - 10^{15} \text{ cm}^{-2}$ (Gaubas et al., 2005) and of neutron-irradiated Si wafers in the range of $10^{12} - 3 \times 10^{16} \text{ cm}^{-2}$ (Gaubas et al., 2008). Again, the lifetimes obtained in this study coincide well with those in the literature, and the lifetimes of neutron-irradiated Si wafers coincide with those of proton-irradiated Si samples. Different slopes were determined by Gaubas et al. (2005) from a linear approximation, i.e., $\tau^{-1} \propto \Phi^{-1/3}$ in the range of low fluences ($10^9 - 4 \times 10^{10} \text{ cm}^{-2}$) and $\tau^{-1} \propto \Phi^{-1}$ in the range of high fluences ($10^{13} - 10^{15} \text{ cm}^{-2}$).

The slope is determined to be ~ 0.77 ($\tau^{-1} \propto \Phi^{-0.77}$) in the range of $10^{10} - 10^{13} \text{ cm}^{-2}$ from the fluence-dependent differences in the reciprocal lifetimes of irradiated and unirradiated Si samples ($\tau^{-1}_{\text{irrad}} - \tau^{-1}_{\text{unirrad}}$) plotted in Fig. 3(b). Considering that τ^{-1} is roughly proportional to the radiation defect density, this result implies that the defect formation rates vary with fluence, and at least three different rate values are present in the fluence range of $10^9 - 10^{15} \text{ cm}^{-2}$.

From the measurements of the DLTS spectra evolution with fluence (Višniakov et al., 2008), it was revealed that point radiation defects such as V-O and divacancies are dominant in low fluence ($7 \times 10^{12} \text{ cm}^{-2}$) proton-irradiated Si wafers. DLTS peaks attributed to V-O and divacancies faded away and a peak associated with vacancy clusters prevailed as fluence increased to $7 \times 10^{14} \text{ cm}^{-2}$. This was attributed to a conglomeration of the point defects into clusters with the enhancement of fluence. This indicates that type and dominance of the radiation defects change with irradiation fluence.

Note that the absolute lifetime values of electron-irradiated Si material are significantly different from proton-irradiated Si at a fixed fluence as shown in Fig. 3(a). This difference in lifetime values were attributed to the larger density of divacancies in proton-irradiated Si, although the type of radiation defects dominated in the electron-irradiated Si was the same with the low fluence proton-irradiated Si, i.e., the point defects such as V-O and divacancies (Višniakov et al., 2008). This implies that the radiation-induced defects change in the type and density with irradiation fluence and particle species (electron vs. proton/neutron).

The changes in resistivity measured by eddy current in μ -PCD are shown in Fig. 4(a) for neutron irradiation. The resistivity was unaffected by the neutron irradiation fluence. The sheet resistance of neutron-irradiated n-type Si wafers measured by the four-probe method also shows negligible change with neutron fluence in the range of $10^8 - 10^{11} \text{ cm}^{-2}$, as shown in Fig. 4(b). The sheet resistance of proton-irradiated Si samples shows that, at fluences higher than 10^{12} cm^{-2} , the resistance increases with fluence.

As was discussed by Liao et al. (2003), large increases in resistivity for proton-irradiated Si wafers were induced by reduction in both the carrier number and mobility. Carrier trapping by proton-induced defects can lead to the decrease in free carriers, and Coulomb scattering of the remaining carriers by the charged trap centers can lead to degradation of the carrier mobility. It was also shown that proton-induced increases in resistivity of lightly doped Si wafers are much more severe than those of heavily doped Si wafers. The threshold proton fluence is 10^{12} cm^{-2} for increase in resistance of the Si wafers with doping concentration of $10^{15} - 10^{16} \text{ cm}^{-3}$ used in this study, whereas resistivity was increased above 10^{15} cm^{-2} proton fluence for Si wafers with doping concentration of $2 \times 10^{18} \text{ cm}^{-3}$ (Liao et al. 2003).

Fig. 5(a) shows the lifetime mappings of neutron-irradiated Si wafers

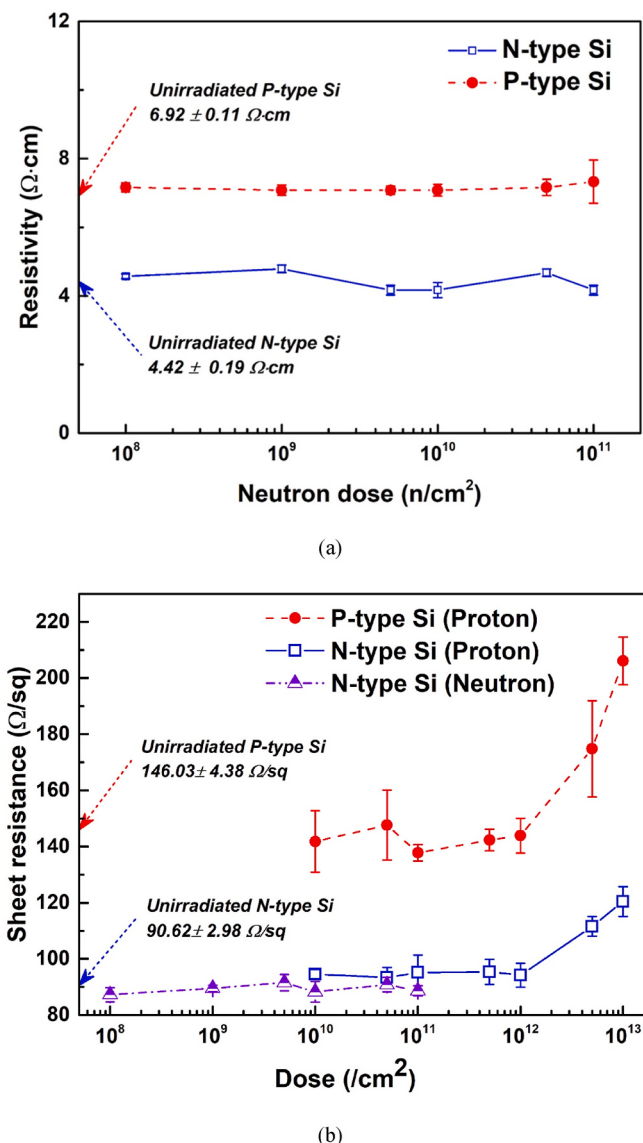


Fig. 4. (a) Resistivity variation of neutron-irradiated Si wafers with neutron fluence and (b) sheet resistance variation of proton-irradiated Si and neutron-irradiated n-type Si wafer with irradiation fluence.

in monochrome colors. As the influence increases, two-dimensional images of IGBT devices located 20 cm in front of the wafers become apparent. The device geometry used in this study is shown in Fig. 5(b). The device is covered by a plastic cap with a hole in the middle and has three protruding terminals from a metal base made of aluminum. The total device thickness is 5 mm. The three terminals can barely be recognized from the lifetime mappings because aluminum is almost transparent to neutrons. The plastic caps are observed with greater contrast because the Si area shaded by the devices was irradiated by less neutrons owing to the scattering of neutrons with plastic, which has a high hydrogen content, inducing a longer lifetime in the shaded area.

The scattering effect on the lifetime is quantified from a line scan on a line passing through the holes of the IGBT devices, as shown in Fig. 5(c), for a p-type wafer irradiated to $1 \times 10^{11} \text{ n/cm}^2$. An exemplary lifetime line scan is shown in Fig. 5(d). The line scan displays periodic ups and downs. The difference in lifetime at the center of a hole and at the location beside the hole is measured as shown in Fig. 5(d) and averaged. The averaged differences in the lifetime ($\Delta\tau$) first increase and then decrease with the neutron fluence, as shown in Fig. 5(e). However, the difference in reciprocal lifetime at the hole and the adjacent covered

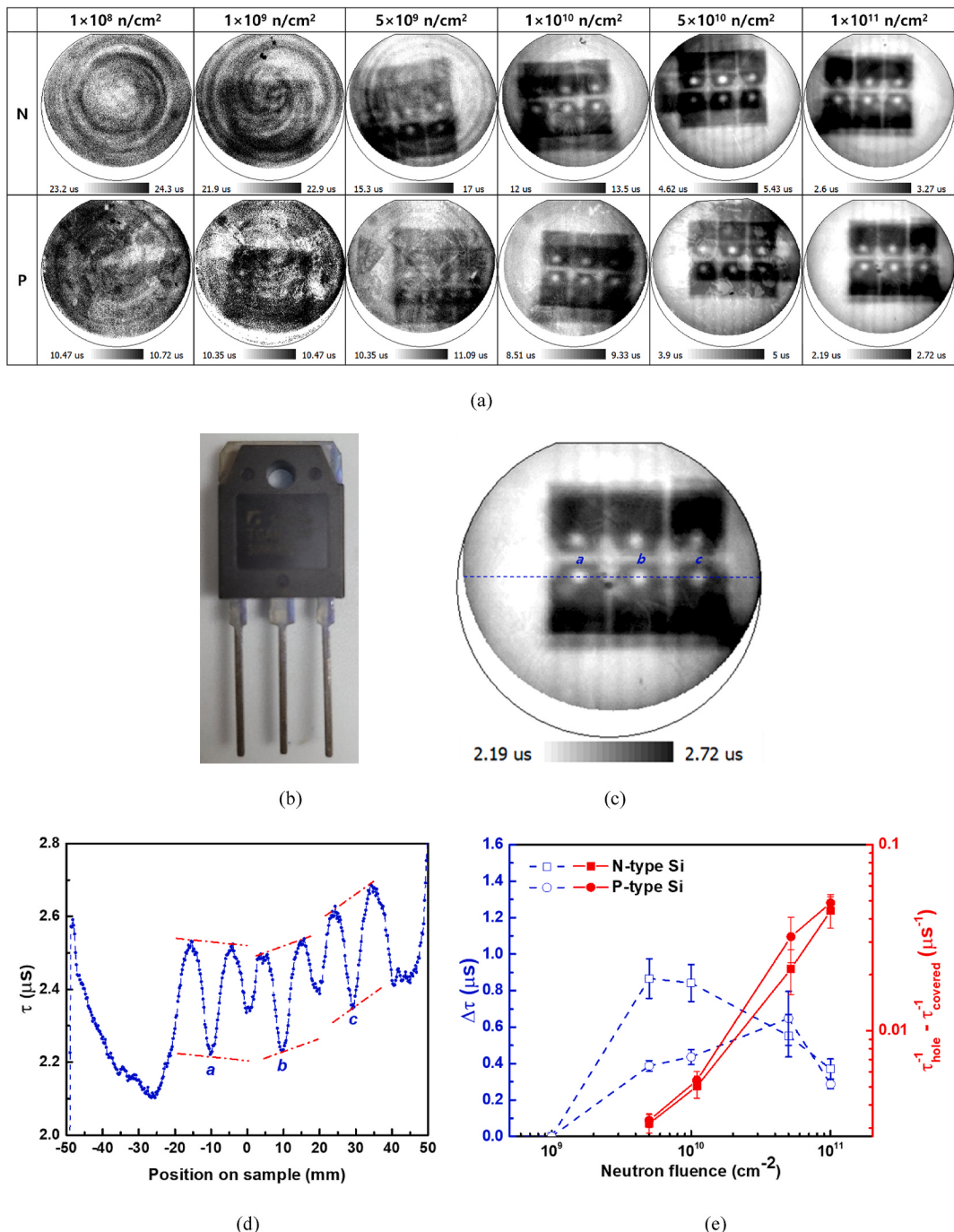


Fig. 5. (a) Monochrome lifetime mappings of neutron-irradiated n- and p-type Si wafers. (b) IGBT device placed in front of Si wafers. (c) Lifetime mapping of p-type Si wafer irradiated to $1 \times 10^{11} \text{ n/cm}^2$. (d) Line scan of the lifetime mapping of (c). (e) The averaged differences in lifetime ($\Delta\tau$) between a hole and an adjacent covered location as a function of neutron fluence along with reciprocal lifetime difference ($\tau_{\text{hole}}^{-1} - \tau_{\text{covered}}^{-1}$).

location ($\tau_{\text{hole}}^{-1} - \tau_{\text{covered}}^{-1}$) increased with increasing neutron fluence. Such change in the lifetime can be taken advantage of in dosimetry of low fluence neutron irradiation.

4. Conclusions

The carrier lifetimes were evaluated using the μ -PCD method in n- and p-type Si irradiated by neutrons and protons in the fluence range of $10^8 - 10^{11} \text{ cm}^{-2}$ and $10^{10} - 10^{13} \text{ cm}^{-2}$, respectively. Unirradiated n-type Si had a longer lifetime than unirradiated p-type Si. The lifetimes of neutron- and proton-irradiated Si exhibited similar irradiation fluence

dependency, manifesting the formation of similar density and types of radiation defects (recombination centers). The defect formation rates vary with irradiation fluence, and at least three different rate values were revealed in the fluence range of $10^9 - 10^{15} \text{ cm}^{-2}$ from the inverse lifetime dependence on irradiation fluence. The resistance of the irradiated Si was unchanged up to a fluence of 10^{12} cm^{-2} and then increased with irradiation fluence. The IGBT devices located 20 cm in front of the Si wafers during neutron irradiation left their images on the lifetime mapping of each Si wafer because of significant neutron scattering by the plastic cap of the devices. The results of fluence-dependent lifetime changes of Si wafers have strong potential for practical use. For example,

in quantifying neutrons as low-dose dosimeters and in fine-tuning the performance of power semiconductors combined with the fluence-dependent resistivity change.

Author statement

Hani Baek: Methodology, Data Curation, Investigation
Gihyun Kwon: Methodology, Data Curation, Investigation
Jongsuk Nam: Visualization, Writing - Review & Editing
Sangeun Kim: Visualization
Hyounghae Kim: Visualization
Byung-Gun Park: Writing - Review & Editing
Jungil Lee: Writing - Review & Editing
Minyoung Kang: Writing - Review & Editing
Gwang Min Sun: Conceptualization, Investigation, Funding acquisition, Writing - Review & Editing
Chansun Shin: Conceptualization, Methodology, Data Curation, Investigation, Writing - Original Draft, Writing - Review & Editing

Declaration of competing interest

The authors declare that they have no known competing financial interests or personal relationships that could have appeared to influence the work reported in this paper.

Acknowledgments

This work was supported by a National Research Foundation of Korea (NRF) grant funded by the government of Korea (MSIP) (2017M2A8A1067400, 2020R1F1A1071092).

References

- Abbaci, M., Meglali, O., Saim, A., Osmani, N., Doghmane, N., 2006. The effect of neutron irradiation defects on electrical resistivity in FZ-silicon samples irradiated at Es-Salam research reactor. *Nucl. Instrum. Methods Phys. Res. B* 251, 167–170.
- Baek, H.N., Sun, G.M., Kim, J.S., Hoang, S.M., Jin, M.E., Ahn, S.H., 2017. Improvement of switching speed of a 600-V nonpunch-through insulated gate bipolar transistor using fast neutron irradiation. *Nucl. Eng. Technol.* 49, 209–215.
- Basore, P.A., Hansen, B.R., 1990. Microwave-detected photoconductance decay, 1. IEEE Conference on Photovoltaic Specialists, Kissimmee, FL, USA, pp. 374–379.
- Bin, Z., Yongqi, C., Peiqing, W., Dongguang, W., 1993. Minority carrier lifetime control in power semiconductor devices by fast neutron irradiation. *Radiat. Phys. Chem.* 42, 1011–1014.
- Brotherton, S.D., Bradley, P., 1982. Defect production and lifetime control in electron and γ -irradiated silicon. *J. Appl. Phys.* 53, 5720.
- Cuevas, A., Macdonald, D., 2004. Measuring and interpreting the lifetime of silicon wafers. *Sol. Energy* 76 (1–3), 255–262.
- Eikelboom, J.A., Leguijt, C., Frumau, C.F.A., Burgers, A.R., 1995. Microwave detection of minority carriers in solar cell silicon wafers. *Sol. Energy Mater. Sol. Cells* 36, 169–185.
- Fujihira, C., Morin, M., Hashizume, H., Friedt, J., Nakai, Y., Hirose, M., 1993. Carrier lifetime measurements by microwave photoconductive decay method at low injection levels. *Jpn. J. Appl. Phys.* 32, L1362–L1364.
- Gaubas, E., Vaitkus, J., Niaura, G., Häkkinen, J., Tuovinen, E., Luukka, P., Fretwurst, E., 2005. Characterization of carrier recombination and trapping processes in proton irradiated silicon by microwave absorption transients. *Nucl. Instrum. Methods Phys. Res. A* 546, 108–112.
- Gaubas, E., Kadys, A., Uleckas, A., Vaitkus, J., 2008. Investigation of carrier recombination in Si heavily irradiated by neutrons. *Acta Phys. Pol. A* 113, 829–832.
- Gaubas, E., Ceponis, T., Uleckas, A., Vaitkus, J., Räisänen, J., 2010. Recombination characteristics in 2–3 MeV protons irradiated FZ Si. *Nucl. Instrum. Methods Phys. Res. A* 612, 559–562.
- Huhtinen, M., 2002. Simulation of non-ionising energy loss and defect formation in silicon. *Nucl. Instrum. Methods Phys. Res. A* 491, 194–215.
- Kumar, R.J., Borrego, J.M., Gutmann, R.J., Jenny, J.R., Malta, D.P., Hobgood, H.McD., Carter Jr., C.H., 2007. Microwave photoconductivity decay characterization of high-purity 4H-SiC substrates. *J. Appl. Phys.* 102, 013704.
- Lauer, K., Laades, A., Übensee, H., Metzner, H., Lawerenz, A., 2008. Detailed analysis of the microwave-detected photoconductance decay in crystalline silicon. *J. Appl. Phys.* 104, 104503.
- Liao, C., Liu, M.-N., Juang, K.-C., 2003. Crosstalk suppression in mixed-mode ICs by the π technology and the future with an SOC integration platform: particle-beam stand (PBS). *IEEE Trans. Electron. Dev.* 50, 1–5.
- Rougieux, F.E., Kwapił, W., Heinz, F., Siriwardhana, M., Schubert, M.C., 2019. Contactless transient carrier spectroscopy and imaging technique using lock-in free carrier emission and absorption. *Sci. Rep.* 9, 14268.
- Schroder, D.K., 1997. Carrier lifetimes in silicon. *IEEE Trans. Electron. Dev.* 44, 160–170.
- Shin, J.W., Bak, S.I., Ham, C.M., J, E., Kim, D.Y., Min, K.J., Zhou, Y., Park, T.S., Hong, S. W., Bhoraskar, V.N., 2015. Neutron spectra produced by 30, 35 and 40 MeV proton beams at KIRAMS MC-50 cyclotron with a thick beryllium target. *Nucl. Instrum. Methods Phys. Res. Sect. A* 797, 304–310.
- Väinölä, H., Saarnilehto, E., Yli-Koski, M., Haarahiltunen, A., Sinkkonen, J., Berenyi, G., Pavelka, T., 2005. Quantitative copper measurement in oxidized p-type silicon wafers using microwave photoconductivity decay. *Appl. Phys. Lett.* 87, 032109.
- Višniakov, J., Gaubas, E., Ceponis, T., Uleckas, A., Räisänen, J., Väyrynen, S., 2008. Comparative investigation of recombination characteristics in proton and electron irradiated Si structures. *Lith. J. Phys.* 48 (2), 137–144.
- Ziegler, J.F., Biersack, J.P., Littmark, U., 1985. The Stopping and Range of Ions in Solids. Pergamon.